# Generation of an astronomical optical frequency comb in three fibre-based nonlinear stages

J. M. Chavez Boggio, A. A. Rieznik, M. Zajnulina, M. Böhm, D. Bodenmüller, et al.

J. M. Chavez Boggio, A. A. Rieznik, M. Zajnulina, M. Böhm, D. Bodenmüller, M. Wysmolek, H. Sayinc, Jörg Neumann, Dietmar Kracht, R. Haynes, M. M. Roth, "Generation of an astronomical optical frequency comb in three fibre-based nonlinear stages," Proc. SPIE 8434, Nonlinear Optics and Applications VI, 84340Y (10 May 2012); doi: 10.1117/12.922538

SPIE.

Event: SPIE Photonics Europe, 2012, Brussels, Belgium

# Generation of an astronomical optical frequency comb in three fibre-based nonlinear stages

J.M. Chavez Boggio[a], A.A. Rieznik[b], M. Zajnulina[a], M. Böhm[c], D. Bodenmüller[a], M. Wysmolek[de], H. Sayinc[de], Jörg Neumann[de], Dietmar Kracht[de], R. Haynes[a], and M.M. Roth[a]

[a]innoFSPEC-VKS, Leibniz-Institut für Astrophysik, An der Sternwarte 16, D-14482 Potsdam, Germany
[b]Instituto Tecnologico de Buenos Aires and CONICET, Buenos Aires, Argentina.
[c]innoFSPEC-InFaSe, University of Potsdam, Physikalische Chemie, Karl-Liebknecht-Str. 24-25, Haus 25, D-14476 Golm, Germany
[d]Laser Zentrum Hannover e.V., Hollerithallee 8, D-30419 Hannover, Germany
[e]Centre for Quantum Engineering and Space-Time Research- QUEST, Welfengarten 1, D-30167 Hannover, Germany

## ABSTRACT

The generation of a broadband optical frequency comb with 80 GHz spacing by propagation of a sinusoidal wave through three dispersion-optimized nonlinear stages is numerically investigated. The input power, the dispersion, the nonlinear coefficient, and lengths are optimized for the first two stages for the generation of low-noise ultra-short pulses. The final stage is a low-dispersion highly-nonlinear fibre where the ultra-short pulses undergo self-phase modulation for strong spectral broadening. The modeling is performed using a Generalized Nonlinear Schrodinger Equation incorporating Kerr and Raman nonlinearities, self-steepening, high-order dispersion and gain.
In the proposed approach the sinusoidal input field is pre-compressed in the first fibre section. This is shown to be necessary to keep the soliton order below ten to minimize the noise build-up during adiabatic pulse compression, when the pulses are subsequently amplified in the next fibre section (rare-earth-doped-fibre with anomalous dispersion). We demonstrate that there is an optimum balance between dispersion, input power and nonlinearities, in order to have adiabatic pulse compression. It is shown that the intensity noise grows exponentially as the pulses start to be compressed in the amplifying fibre. Eventually, the noise decreases and reaches a minimum when the pulses are maximally compressed. A train of 70 fs pulses with up to 3.45 kW peak power and negligible noise is generated in our simulations, which can be spectrally broadened in a highly-nonlinear fibre. The main drawback of this compression technique is the small fibre length tolerance where noise is negligible (smaller than 10 cm for erbium-doped fibre length of 15 m). We finally investigate how the frequency comb characteristics are modified by incorporating an optical feedback. We show that frequency combs appropriate for calibration of astronomical spectrographs can be improved by using this technique.

**Keywords:** Optical frequency comb, Four-wave mixing, pulse compression, Astronomy.

## 1. INTRODUCTION

Since their inception optical frequency combs (OFCs) generated in passively mode-locked lasers have revolutionized the endeavors of metrology, spectroscopy and other scientific areas [1-3]. Even though they can be routinely generated in very compact systems and the comb line spacing can now be up to a few GHz, there are several applications where larger comb spacing are required, up to the THz range. One interesting example of such an application is Astronomy Astronomy – the quest for high-precision wavelength calibration of optical or NIR spectrographs at ground-based or space telescopes has received great attention over the last years because of the potential for ground-breaking discoveries, e.g. a possible change of the fine structure constant over cosmic times [4], the direct measurement of the Hubble constant [5], or the detection of earth-like extra-solar planets [6]. Current state-of-the-art wavelength calibrators are

Nonlinear Optics and Applications VI, edited by Benjamin J. Eggleton, Alexander L Gaeta, Neil G. Broderick,
Proc. of SPIE Vol. 8434, 84340Y · © 2012 SPIE · CCC code: 0277-786X/12/$18 · doi: 10.1117/12.922538

based on the light from low pressure spectral line lamps, providing very few and non-uniformly spaced emission lines with strongly unequal intensities. It has been suggested that an ideal high-precision calibrator should incorporate uniformly spaced and equally intense spectral lines spanning several hundreds of nanometers [6-13]. The use of an optical frequency comb is expected to improve the calibration accuracy, currently limited by the spectral characteristics of conventional spectral line lamps [6]. To generate an astro-comb, researchers have recently used a mode-locked laser followed by a complicated set of stabilized Fabry-Perot cavities to filter out unwanted comb modes. In this way, an OFC with line spacing of 14 GHz has been recently demonstrated, and its capabilities for the calibration of high-resolution spectroscopy were tested at the HARPS spectrograph [13]. However, in order to massively deploy OFCs in telescopes around the world, the degree of complexity, size, and cost needs to be dramatically reduced. In that respect, it was recently demonstrated that a frequency comb can be generated in a high-$Q$ micro-resonator – a laser is launched to match one resonance of the resonator and a cascade of four-wave mixing (FWM) products give rise to a broadband frequency comb [14-21]. However, several issues related to the noise performance and comb stability need to be solved before they reach a mature stage.

In this paper we investigate a simple all-fibre scheme for astronomical optical frequency comb generation. In section II we describe the approach we follow for pulse compression and spectral broadening for the astro-comb generation. We also describe the details of the Generalized Nonlinear Schrodinger Equation that was solved numerically. Section III, IV, and V describe our results for the first, second and third nonlinear stage, respectively. Finally, in section VI we draw our conclusions.

## 2. ASTRONOMICAL FREQUENCY COMB GENERATION: THEORETICAL FRAMEWORK

Figure 1 shows the schematic of the nonlinear system we are proposing to generate the astronomical optical frequency comb. It consists of two phase-locked and equally intense lasers (with frequencies $\omega_1$ and $\omega_2$) that are propagated through three nonlinear stages. The two-tone initial field corresponds temporally to a sinusoidal square pulse that is subject to an initial compression (or pre-chirping) during the propagation in the first fibre segment. The second stage is the amplifying fibre that amplifies the average power and also provides strong (adiabatic) pulse compression. We seek to understand if it is possible to adjust the interplay of dispersion and non-linearities in the first two fibre stages for efficient compression of the initially sinusoidal pulses and with negligible pedestal. The aim is to generate clean sub-100 fs pulses with high repetition rates (>50 GHz) that would have enough peak power for subsequent generation of astronomical optical frequency combs in a low-dispersion nonlinear fibre.

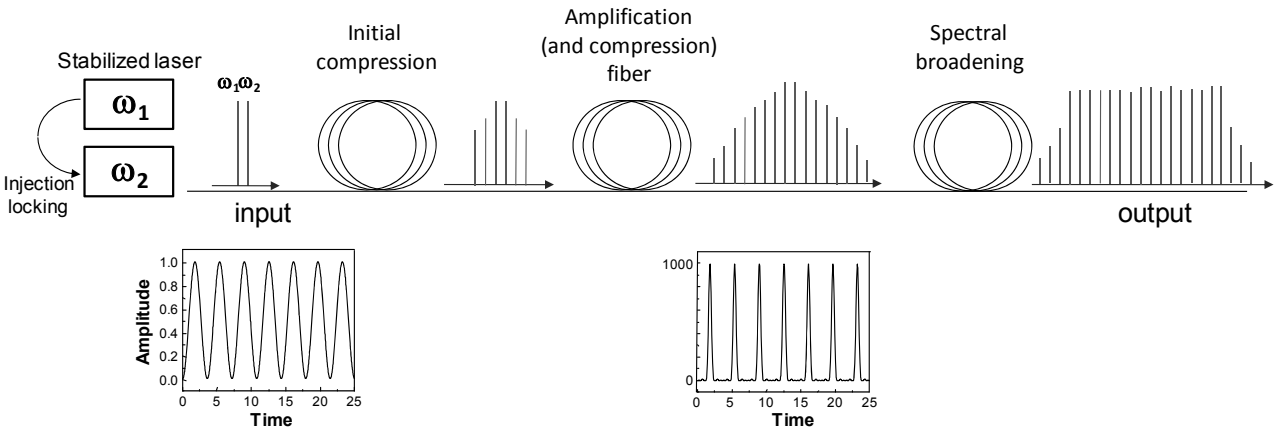


Figure 1. Schematic of the proposed pulse compression approach.

To investigate the system described in Fig. 1, we consider the two-laser optical field described by

$$A_0(z,t) = \sqrt{P_0}\,\sin(t/\tau)e^{i(\omega_c t-\beta z)} \quad (1),$$

where $\omega_c = (\omega_1 + \omega_2)/2$ is the central frequency (center wavelength is at 1531 nm), $\beta$ is the wavenumber, $\tau$ is the period of the sinusoidal envelope modulation, $P_0$ is the peak power of the sinusoidal pulse, and $z$ is the propagation distance. The noise characteristics of the pulses are investigated by including a noise contribution to the total field:

$$A = A_0 + \sqrt{n_0}\,e^{i(\omega_c t-\beta z+\varphi_{random})} \quad (2).$$

where $n_0$ is the noise amplitude and $\varphi_{random}$ is a random phase with uniform distribution over $[0, 2\pi]$. The two laser input was generated in two stages, in order to mimic the experimental configuration under development at innoFSPEC. First, the noise level is set 65 dB lower than the laser level. Then 30 GHz band-pass filters are used to filter out further the noise background. In this way the optical-signal-to-noise-ratio (OSNR) is 80 dB. The propagation of this field along the three nonlinear stages depicted in Fig. 1 is numerically investigated by solving the Generalized Nonlinear Schrodinger Equation (GNLSE) in the frequency domain using the split step Fourier method. The GNLSE is given by

$$\frac{\partial\tilde{A}(\Omega)}{\partial z} + i\frac{\alpha(\Omega)}{2}A(\Omega) + i\tilde{A}(\Omega)\beta(\Omega) = -i\gamma\left(1+\frac{\Omega}{\omega_0}\right)\times\left(F\left[(1-f_R)\right]\tilde{A}(\Omega)\left|\tilde{A}(\Omega)\right|^2 + f_R\,\tilde{A}(\Omega)F^{-1}\left[h_R F\left[\left|\tilde{A}(\Omega)\right|^2\right]\right]\right) \quad (3)$$

where $\tilde{A}(z,\Omega)$ as the Fourier transform of $A(z,t)$, $\alpha$ is the fiber gain coefficient, the propagation constant $\beta(\omega)$ around the carrier frequency $\omega_c$, $\gamma$ is the nonlinear coefficient of the fiber fundamental mode, $R(t) = (1-f_R)\delta(t) + f_R h_R(t)$, and $0 < f_R < 1$ represents the fractional contribution of the delayed Raman response $h_R$, which is given by

$$\begin{aligned} h_R(t) &= (f_a + f_c)h_a(t) + f_b h_b(t), \\ h_a(t) &= \tau_1\left(\tau_1^{-2} + \tau_2^{-2}\right)\exp(-t/\tau_2)\sin(t/\tau_1), \\ h_b(t) &= \left[\left(2\tau_b - t\right)/\tau_b^2\right]\exp(-t/\tau_b), \end{aligned} \quad (4)$$

where $\tau_1 = 12.2$ fs , $\tau_2 = 32$ fs, $\tau_b = 96$ fs, $f_a = 0.75$, $f_b = 0.21$, $f_c = 0.04$, and $f_R = 0.24$ [2]. We defined $\Omega = \omega - \omega_c$, $F$ stands for direct Fourier transform, $F^{-1}$ for the inverse transform, and $\tilde{h}_R = F(h_R(t))$. Numerically, $F$ and $F^{-1}$ are computed using the fast Fourier transform (FFT) and inverse FFT (IFFT), respectively.

## 3. NUMERICAL RESULTS: COMB GENERATION IN A SINGLE PASS

### 3.1 FIRST STAGE: PRE-COMPRESSION

The GNLSE was numerically solved for the fibre propagation of the field at Eq. (2) for the case when the two lasers are 80 GHz apart and with input powers that can vary from $P_0 = 0.4$ to 10 W. Two values of the fibre nonlinear coefficient are considered in our analysis: $\gamma = 2$ and $\gamma = 10$ (W-km)$^{-1}$; while the second order dispersion is scanned from $\beta_2 = -30$ to -5 ps$^2$/km. The third order dispersion is set at $\beta_3 = 0.1$ ps$^3$/km. Figure 2 shows the calculation results for the peak power of the pulse train as a function of the propagation length for the case $P_0 = 1$ W and for several $\beta_2$ values. Note that as the pulse propagates, its peak power increases and then reaches a maximum value and finally decreases. This power increase is due to pulse compression caused by solitonic self-adjustment of the pulse width [20]. In the frequency domain the pulse compression is manifested as spectral broadening: initially the two lasers interact by four-wave mixing (FWM) and generate phase-locked sidebands which then further interact to generate a cascade of new spectral products. At some point during the propagation, the amount of new spectral sidebands generated by FWM reach a maximum (consequently the compression attains a maximum too) and after that the power flow from pumps to sidebands is reversed and the peak power starts to decrease. Figure 2(a) shows the results for $\gamma = 2$ (W-km)$^{-1}$ while Figure 2(b) shows the case $\gamma = 10$ (W-km)$^{-1}$, revealing a similar behavior in both cases. However, the compression ratio increases as $\gamma$ increases or $\beta_2$ decreases: for example, the propagation of a train of pulses with 1W of initial peak power grows to 12W after propagation through 0.45 km of a fibre with $\gamma = 10$ (W-km)$^{-1}$ and $\beta_2 = -6$ ps$^2$/km; this means a compression factor of 12.

This fibre was cut at the length of maximum compression and the optical field at this position is then propagated through the second fibre (the amplifying medium). Note that by changing the fibre dispersion and/or the nonlinearity we are not only changing the peak power that is entering the amplifying medium but also the pulse width and the chirp of the pulses. These changes in the input characteristics will affect the dynamics in the next nonlinear stage.

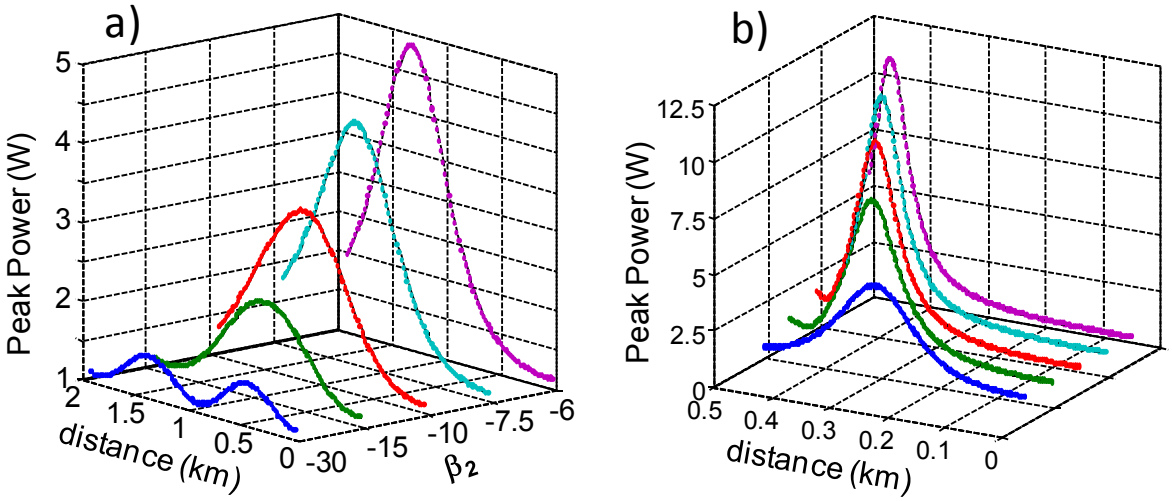


Figure 2. Peak power as a function of propagation length when $P_0$ = 1 W and for $\beta_2$ = -30, -15, -10, -7.5, -6 ps$^2$/km. (a) $\gamma$ = 2 (W-km)$^{-1}$ and (b) $\gamma$ = 10 (W-km)$^{-1}$.

### 3.2 SECOND STAGE: AMPLIFICATION AND STRONG (ADIABATIC) COMPRESSION

By propagating the pulses through the amplifying fibre, the aim is not only to increase the average power but by judiciously adjusting the gain and anomalous dispersion to induce strong pulse compression in order to reach the necessary peak power for broadband frequency comb generation.

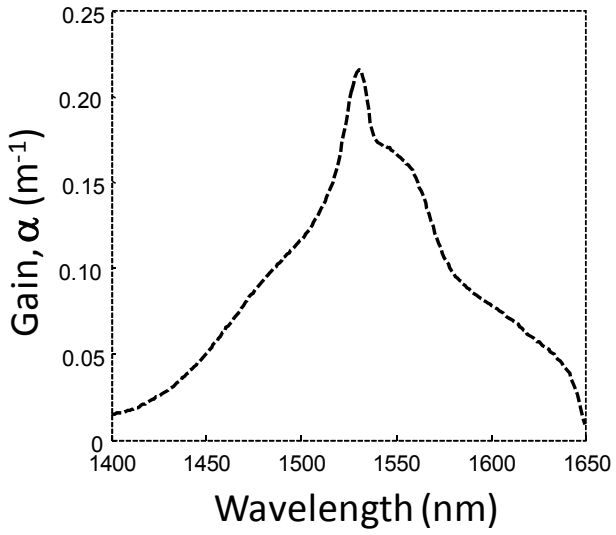


Figure 3. Spectrum of the gain coefficient ($\alpha$) of the amplifying fibre.

The spectral characteristics of the gain coefficient of the amplifying fibre used in our calculations are shown in Figure 3. The gain has the typical shape of an Erbium doped fibre. The other important parameters of the fibre are the second and third order dispersion with values $\beta_2 = -14$ ps$^2$/km, $\beta_3 = 0.1$ ps$^3$/km, respectively; and the nonlinear coefficient $\gamma = 2.5$ /W-km.

The peak power of the pulses as a function of the propagation length in the amplifying fibre was calculated for the case when the first fibre has $\gamma = 2$ (W-km)$^{-1}$ and $\beta_2 = -30, -15, -10, -7.5, -6$ ps$^2$/km and the power injected in this fibre was $P_0 = 1$ and 2.5 W. Figure 4 shows the peak power as the pulses propagated through the amplifying fibre. It can be observed that in the first meters of propagation the peak power increases slowly (almost entirely due to the amplification process and not to any compression effect). When the pulses (or the spectral sidebands) reach enough power to generate more cascaded FWM tones, the pulses start to experience significant compression and the peak power increases rapidly from less than 0.3 kW to a few kW. When the peak power reaches its maximum, the phase relationship between the different spectral components changes its sign and the power flow is reverted producing pulse broadening and the peak power decreases. As the amplifier continues to provide energy to the pulses, there will be again generation of new spectral components due to FWM and the peak power will have an oscillatory behavior with a tendency of peak power increasing as the pulses propagate further in the amplifying medium. A close inspection of Fig. 4 shows that the peak power at the first maximum is higher as the first fibre has a larger $\beta_2$ or as the input power $P_0$ is smaller – both cases result in a smaller power that enters the amplifier. Note also that when the input power at the second fibre is smaller, the amplifier needs more length (gain) to compress the pulses and reach the first maximum. More importantly the peak power increase is steeper which can make it difficult to properly setup this compressor section.

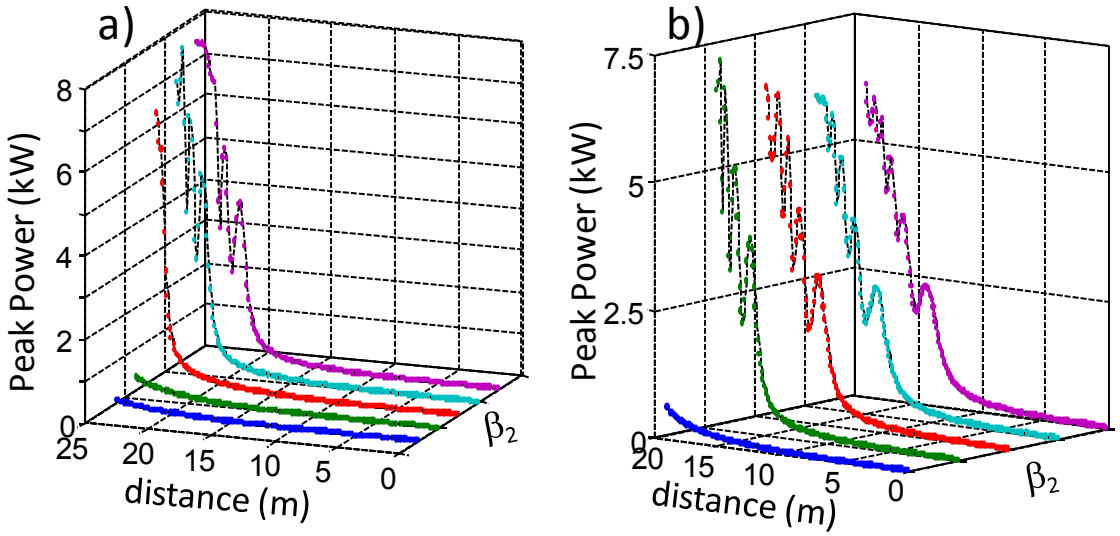


Figure 4. Peak power as a function of the propagation length in the amplifying medium for $\gamma = 2$ (W-km)$^{-1}$, $\beta_2 = -30, -15, -10, -7.5, -6$ ps$^2$/km of the first fibre and for (a) $P_0 = 1$ W and (b) $P_0 = 2.5$ W.

The noise characteristics of the optical frequency comb will be dictated by the quality of the pulses generated in the amplifying medium. To assess the noise characteristics of the train of pulses we have calculated its relative intensity noise (RIN). The RIN was defined as the ratio between the pulse with the highest peak power and the average peak power in the train of pulses. Since the simulation time window is 256 ps, the calculation was done for a train of pulses consisting of 20 pulses (period $\tau = 13$ ps). The noise intensity results corresponding to Figure 4 are shown in Figure 5. As with the peak power, the intensity noise increases as the pulse propagates along the fibre, reaches a maximum but decreases to a minimum value for a length that corresponds exactly to the length when the peak power reaches a maximum. A comparison of Figures 5(a) and 5(b) shows that the RIN is smaller for smaller $\beta_2$ of the first fibre and for larger input powers. This indicates that there is a range of peak power values and pulse widths entering the amplifying fibre that minimize pulse intensity noise: the lowest noise is obtained when the amplifying fibre provides moderate

compression ratios rather than large ones. This behaviour is explained in terms of pulse compression of high-order solitonic pulses. In order to have a gentle compression, the order ( $N = \sqrt{\frac{\gamma P T_0^2}{|\beta_2|}}$ ) of the solitonic pulse needs to be smaller than 10. The larger the soliton order is, the higher will be the compression ratio but the compression will not be adiabatic, and the non-adiabaticity will lead to the formation of a strong pedestal around the pulse. If the soliton order becomes too high (>10), the interaction of the pulse with the pedestal can result in pulse break-up (soliton fission).

We checked that at maximum compression the pulses have a width smaller than 80 fs in most of the cases, which means a compression factor of 80 (from the initial 6.3 ps of the sinusoidal square wave). However, it is also noted that the pedestal carries more than 20 % of the total power. After the first maximum, the pulses are further amplified and will become noisier and unstable since the soliton order will continue to grow as the power increases. Therefore, the pulses will undergo soliton fission into several pulse components (the powerful spectral components will interact with the background noise) and the RIN will increase prohibitively.

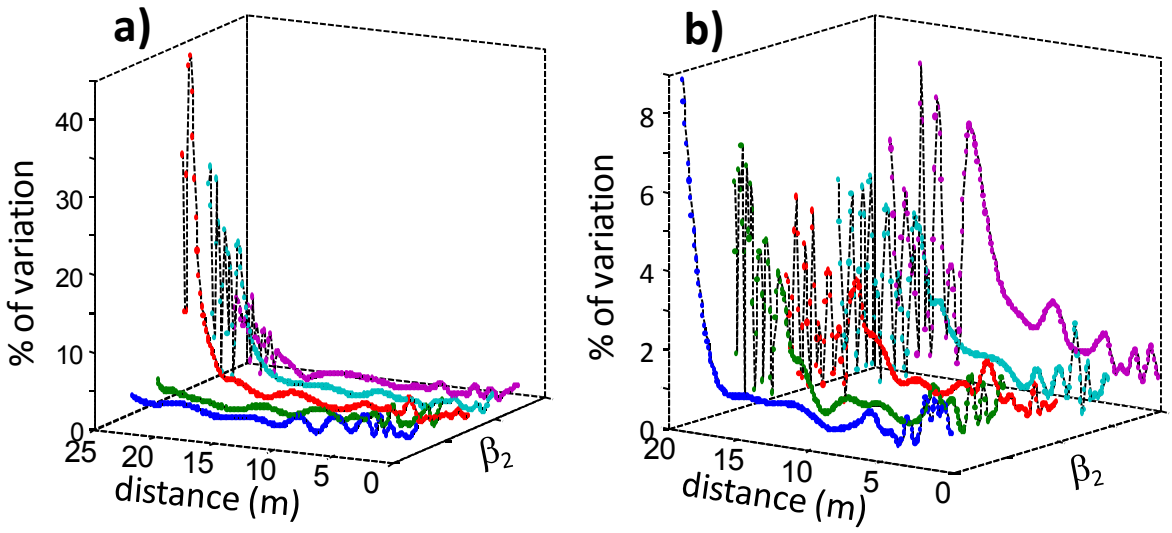


Figure 5. Intensity noise as a function of the propagation length in the amplifying medium for $\gamma = 2$ (W-km)$^{-1}$, $\beta_2$ = -30, -15, -10, -7.5, -6 ps$^2$/km of the first fibre and for (a) $P_0 = 1$ W and (b) $P_0 = 2.5$ W.

### 3.3 THIRD STAGE: FREQUENCY BROADENING

We have cut the amplifying fibre segment at the length where we have the first maximum compression and propagate the compressed pulses through the third and last fibre segment having a length of $L = 1$ m, $\beta_2 = 0.05$ ps$^2$/km, $\beta_3 = 0.0081$ ps$^3$/km, and $\gamma = 10$ (W-km)$^{-1}$. We chose the case when the train of pulses compressed in the amplifying medium had a peak power of 3.45 kW (corresponding to $P_0 = 2.5$ W, for $\gamma = 2$ (W-km)$^{-1}$ and $\beta_2 = -15$ ps$^2$/km for the first fibre) and the result is shown in Figure 6.

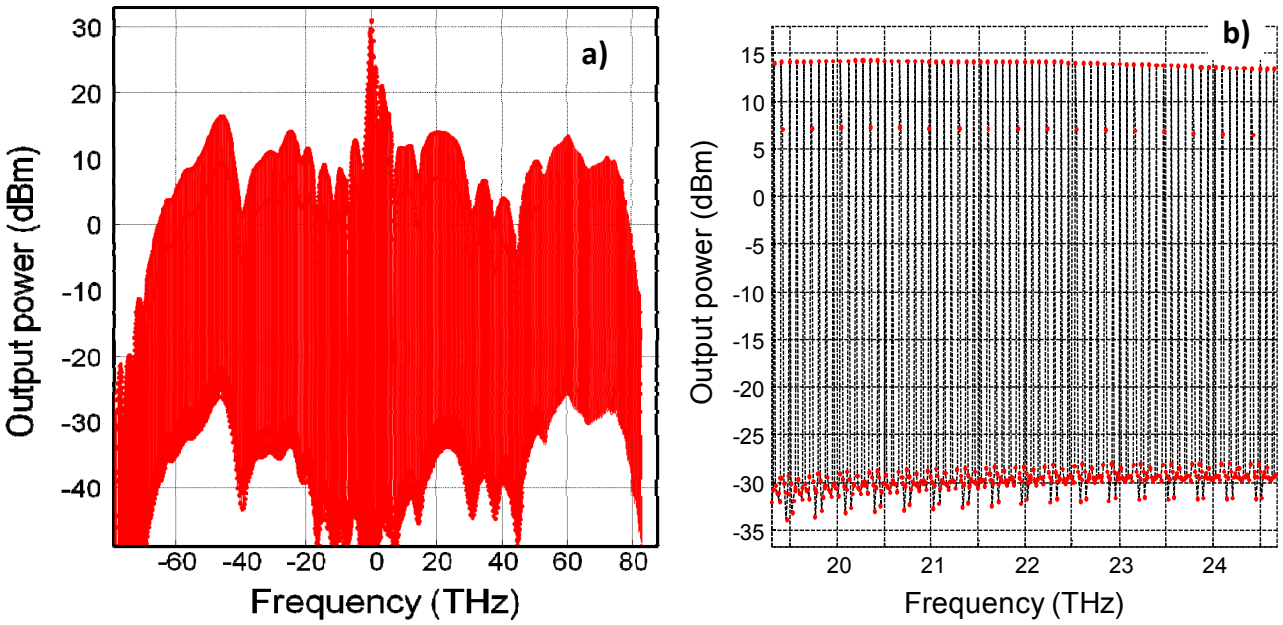


Figure 6. Output spectrum after third nonlinear stage having $L$ = 1 m. (a) Whole comb spectrum spanning 145 THz. (b) Zoom showing the frequency range between 20 and 25 THz.

The optical frequency comb extends over a bandwidth of 145 THz (one octave spanning) and this is a respectable bandwidth for this relatively low peak power. The optical signal to noise ratio (OSNR) is ~ 40 dB for nearly the entire comb. Even though the power carried by each comb tooth is not equalized along the 145 THz (power variation is 20 dB), our results are a significant step forward for the understanding of frequency comb generation at large comb spacing.

## 4. NUMERICAL RESULTS: COMB GENERATION WITH A FEEDBACK

The dynamics of frequency comb generation in a nonlinear medium might be drastically changed by placing the medium in a loop [22]. To study how an optical feedback can improve the characteristics of an OFC, we analyse the simple system shown in Figure 7. It consists of two lasers that are combined in a fibre and then propagated through a nonlinear fibre. Lossless couplers are used to form a loop, where some percentage of the power is reinserted to the input (point B).

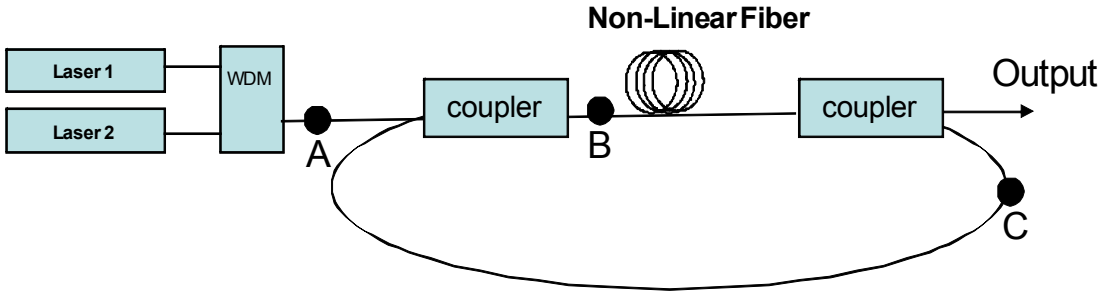


Figure 7. Simplest configuration for optical frequency comb generation in a fibre loop.

To study the advantage of using the fibre loop we compare the number of FWM sidebands with an OSNR larger than 15 dB for the single pass case (i.e. when the loop is open), against the case when the loop is closed with a given reinserted power. We also compare both cases against the single pass case but with an input power as large as the effective power in point B in Figure 7 when the loop is closed and the steady state conditions are reached. The effective peak power in B depends on the reinserted power. Using standard fiber couples one could reinsert over 95% of the output power. Simulations show, however, that no more than 20% of reinsertion is generally optimal because under realistic conditions a broad band noise starts to deteriorate the OSNR at the output. With 20% of reinsertion, the input peak power at B under steady state conditions is 3.3 times larger than the peak power at A.

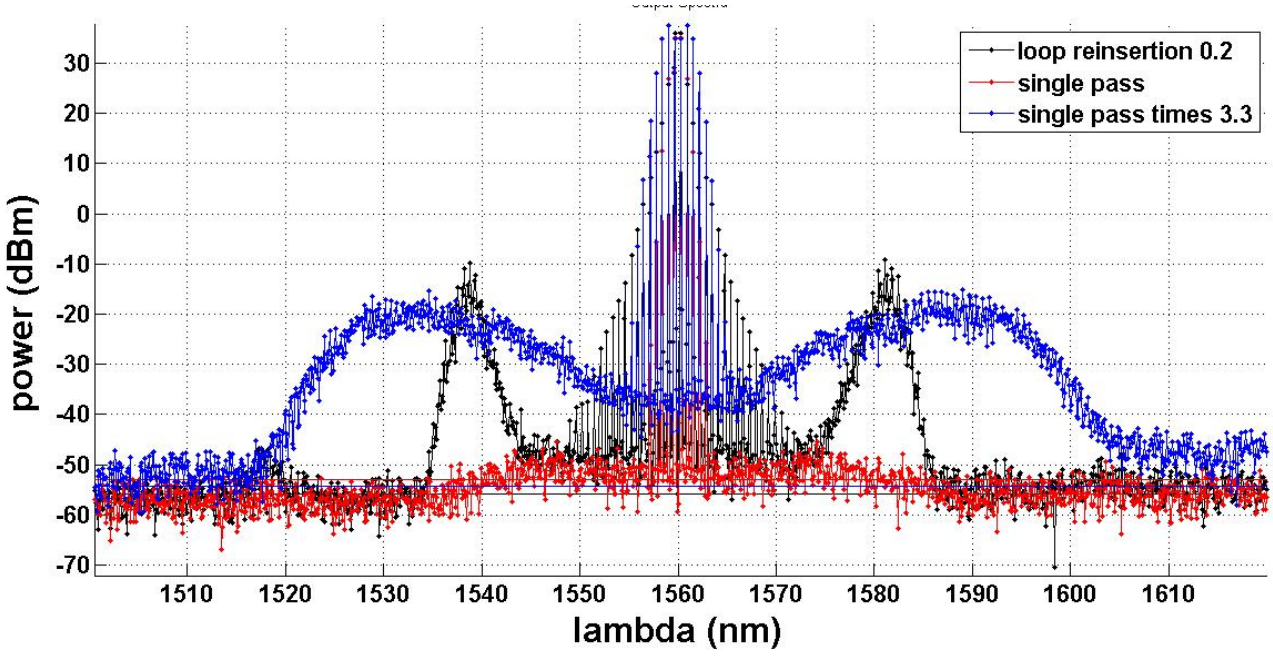


Figure 8. Output spectra: for 2.5 W input peak power, without loop (red) and with a loop with 20% reinserted power (black), and for 8.25 W input peak power (blue).

Figure 8 shows the output spectra for the single pass case with peak powers at point A of 2.5 W and 3.3×2.5 = 8.25 W, for an input peak power of 2.5W, and a closed loop with 20% reinsertion. It is clear from this figure that using the loop is the best option: the number of comb lines with an OSNR larger than 15 dB is 26 in this case, against 10 and 14, for the single pass case with input peak powers of 2.5 and 8.25 W, respectively. We observed that using larger reinsertion powers do not improve the comb because the noise starts to be amplified prohibitively deteriorating the OSNR of the comb lines.

It was also tested if the comb bandwidth could be increased by introducing an optimized phase shift in the loop (in a real experiment this shift can be adjusted by adjusting the length of the feedback loop). Figure 9 shows that the comb bandwidth cannot be increased: for phase shift from 0 to 8000 fs the bandwidth of the comb is almost constant. At larger phase shift the behavior is quite complex but in no case the bandwidth is improved.

An interesting observation is that, depending on the amount of phase shift, we either could, or rather could not achieve a converged numerical solution, respectively. For some phase shifts the spectra at the output converges towards a stable solution or changes significantly at each loop infinitely. This chaotic fractal-like behavior was already observed in [22].

An interesting observation is that depending on the amount of phase shift, the loop could or not achieve a converged numerical solution. For some phase shifts the spectra at the output converges towards a stable solution or changes significantly at each loop infinitely.

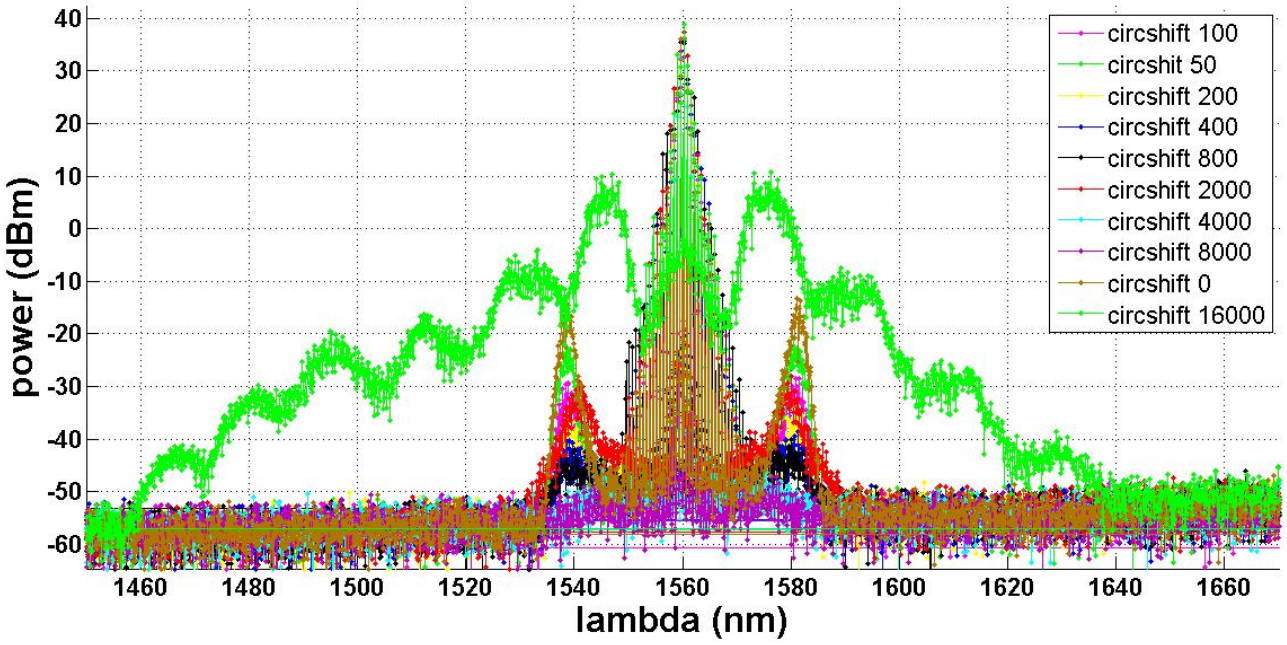


Figure 9. Output spectra for a loop with 20% reinsertion power and 2.5 W input peak power at point A, for different amounts of shift. The shift is given in femto-seconds in the legends.

## 5. CONCLUSIONS

We have numerically investigated the generation of astronomical optical frequency combs in a three-stage nonlinear system. The generation of low-noise ultra-short high-repetition-rate pulses starting from two lasers and using two nonlinear stages with appropriate dispersion and nonlinear characteristics was investigated. The first one serves as an initial compression (pre-chirping) stage, while the second fiber provides gain and simultaneously strong pulse compression down to sub-100 fs. The obtained pulses are shown to be very clean due to the adiabatic compression and are appropriate for subsequent generation of broadband frequency comb spanning nearly one octave. The effect of introducing an optical feedback was also investigated, showing that the number of comb lines can be increased by almost a factor of three. The envisaged next step is to verify these findings and to setup an experiment for the generation of a low-noise broadband astronomical frequency comb.

**Acknowledgment**

We would like to acknowledge the financial support from Federal Ministry of Education and Research (BMBF) for financial support under grants 03Z2AN11 and 03Z2AN12. Fruitful discussions with Bernhard Roth are gratefully acknowledged.

## 6. REFERENCES

[1] D. J. Jones *et al.*, "Carrier–envelope phase control of femtosecond mode-locked lasers and direct optical frequency synthesis", Science 288, 635 (2000).

[2] R. Holzwarth *et al.*, “Optical frequency synthesizer for precision spectroscopy”, Phys. Rev. Lett. 85 (11), 2264 (2000).
[3] S. T. Cundiff and Jun Ye, “Colloquium: femtosecond optical frequency combs”, Rev. Mod. Phys. 75, 325 (2003).
[4] K. Griest et al., “Wavelength Accuracy of the Keck HIRES Spectrograph and Measuring Changes in the Fine Structure Constant,” Astrophys. J., vol. 708, 158-170 (2010).
[5] A. Loeb, “Direct Measurement of Cosmological Parameters from the Cosmic Deceleration of Extragalactic Objects,” Astrophys. J., vol. 499, L111 (1998).
[6] M.T. Murphy et al., “High-precision wavelength calibration of astronomical spectrographs with laser frequency combs,” Mon. Not. R. Astron. Soc., vol. 380, 839-847 (2008).
[7] D. A. Braje, M. S. Kirchner, S. Osterman, T. Fortier and S. A. Diddams, “Astronomical spectrograph calibration with broad-spectrum frequency combs”, Eur. Phys. J. D, vol. 48, 57-66 (2008).
[8] C. H. Li, A. J. Benedick, P. Fendel, A. G. Glenday, F. X. Kärtner, D. F. Phillips, D. Sasselov, A. Szentgyorgyi and R. L. Walsworth, “A laser frequency comb that enables radial velocity measurements with a precision of 1 cm s-1”, Nature, vol. 452, 610-612 (2008).
[9] T. Steinmetz, et al. “Laser frequency combs for astronomical observations,” Science, vol. 321, 1335-1337 (2008).
[10] T. Steinmetz, T. Wilken, C. Araujo-Hauck, R. Holzwarth, T.W. Hänsch and T. Udem, “Fabry–Pérot filter cavities for wide-spaced frequency combs with large spectral bandwidth”, Appl. Phys. B, vol. 96, 251-256 (2009).
[11] T. Wilken, T.W. Hänsch and T. Udem, T. Steinmetz, R. Holzwarth, A. Manescu, G. LoCurto, L. Pasquini, C. Lovis, “High precision calibration of spectrographs in astronomy,” Conference on Lasers and Electro-Optics (CLEO), San Jose, CA, USA (2010) .
[12] T. Wilken, C. Lovis, A. Manescu, T. Steinmetz, L. Pasquini, et al., “High precision calibration of spectrographs,” Mont. Not. R. Astron. Soc., 405, L16-L20 (2010).
[13] A. Manescu, et al., “Approaching cm/s calibration of high resolution astronomical spectrographs,” CLEO-Europe, Munich (2011).
[14] P. Del’Haye, A. Schliesser, O. Arcizet, T. Wilken, R. Holzwarth, and T.J. Kippenberg, “Optical frequency comb generation from a monolithic micro-resonator,” Nature, vol. 450, 1214-1217 (2007).
[15] P. Del'Haye, O. Arcizet, M.L. Gorodetsky, R. Holzwarth, & T.J. Kippenberg, “Frequency comb assisted diode laser spectroscopy for measurement of microcavity dispersion,” Nature Photonics, vol. 3, 529-533 (2009).
[16] P. Del'Haye, O. Arcizet, A. Schliesser, R. Holzwarth, T.J. Kippenberg, “Full stabilization of a microresonator based optical frequency comb,” Physical Review Letters vol. 101, 053903 (2008).
[17] A.A. Savchenkov, et al. "Tunable optical frequency comb with a crystalline whispering gallery mode resonator," Physical Review Letters, vol. 101, 093902 (2008).
[18] J. S. Levy, A. Gondarenko, M. A. Foster, A. C. Turner-Foster, A. L. Gaeta, and M. Lipson, "CMOS-compatible multiple-wavelength oscillator for on-chip optical inter-connects,” Nature Photonics, vol. 4, 37-40 (2009).
[19] M. A. Foster, J. S. Levy, O. Kuzucu, K. Saha, M. Lipson, and A. L. Gaeta, "CMOS-Compatible Microresonator-Based Optical Frequency Comb," in Conference on Lasers and Electro-Optics, OSA Technical Digest (CD) (Optical Society of America, 2010), paper CMHH5 (2010).
[20] A.A. Savchenkov, E. Rubiola, A.B. Matsko, V.S. Ilchenko, and L. Maleki, "Phase noise of whispering gallery photonic hyper-parametric microwave oscillators," Opt. Express, vol. 16, 4130-4144 (2008).
[21] S. M. Spillane, T. J. Kippenberg, and K. J. Vahala, ”Ultra low threshold Raman laser using a spherical dielectric microcavity,” Nature, vol. 415, 621-623 (2002).
[22] Nicoletta Brauckmann, Michael Kues, Petra Groß, and Carsten Fallnich, “Noise reduction of supercontinua via optical feedback,” Optics Express, vol. 19, pp. 14763–14778, Aug. 2011.